Piezoelectric properties of $SrBi_4Ti_4O_{15}$ ferroelectric ceramics

Marlyse Demartin Maeder, Dragan Damjanovic, Cyril Voisard, and Nava Setter
Ceramics Laboratory, Materials Department, Swiss Federal Institute of Technology - EPEL, 1015 Lausanne, Switzerland

(Received 21 June 2001; accepted 14 March 2002)

The dynamic piezoelectric response of $SrBi_4Ti_4O_{15}$ ceramics with Aurivillius structure was investigated at high alternating stress, low frequencies (0.01 to 100 Hz), and temperatures from 20 to 200 °C. The piezoelectric nonlinearity, observed only at high pressures (>10 MPa) and elevated temperatures (>150 °C), is interpreted in terms of contributions from non-180° domain walls. At weak fields, the frequency dependence of the longitudinal piezoelectric coefficient was explained in terms of Maxwell–Wagner piezoelectric relaxation. The Maxwell–Wagner units are identified as colonies that consist of highly anisotropic grains which sinter together, and whose distribution in the ceramic is strongly dependent on sintering conditions.

I. INTRODUCTION

Many compositions that belong to the family of bismuth titanate ($Bi_4Ti_3O_{12}$or BIT) based materials possess a high transition temperature and have been considered for use in high-temperature piezoelectric applications.[1] These materials have recently also attracted considerable attention for potential applications in nonvolatile ferroelectric memories due to their excellent polarization fatigue resistance.[2] Finally, following the current interest in developing lead-free piezoelectric components, bismuth titanate based materials may be of interest as an alternative to conventional lead-based compositions for certain applications.

The crystal structure of these compositions, first described by Aurivillius,[3] is characterized by pseudo-perovskite layers ($A_{m-1}BO_{3m+1}$ stacked between $(Bi_2O_2)^{2+}$ layers.[4] A is a mono, divalent or trivalent cation and B a quadri, penta, or hexavalent metal. The number of perovskite layers is represented by *m*. Due to the layer structure, the compositions exhibit a very high anisotropy of properties.[5] With the known exception of monoclinic BIT, in most Aurivillius phases the structure can be described as orthorhombic below the paraelectric–ferroelectric phase transition temperature, and polarization takes place in the *ab* plane.[6,7] The piezoelectric effect is also highest in this plane. In the ceramics, the microstructure of such materials consists of platelike-shaped grains.[8] For these crystallites, the smallest dimension of the grain corresponds to the crystallographic *c* axis so that the polarization lies in the plane of the grains.

From the point of view of piezoelectric properties, $SrBi_4Ti_4O_{15}$ (SBTO15) is of special interest because of its high Curie temperature (≈530 °C) and its remarkably stable properties with respect to the driving field amplitude and frequency.[9,10] This stability has been discussed using crystallographic arguments by Reaney and Damjanovic.[11] They presented evidence that the ferroelastic and ferroelectric phase transitions in SBTO15 do not occur at the same temperature, as in $BaTiO_3$ and $PbTiO_3$. On cooling, SBTO15 first undergoes a phase transition from a high-temperature tetragonal paraelectric-paraelastic phase into an orthorhombic(I) paraelectric–ferroelastic phase. Observations of electron diffraction patterns by transmission electron microscopy reveal the presence of superlattice reflections associated with this phase transition.[11] Suppelattice reflections are observed below 650–680 °C, suggesting that the phase transition occurs in this temperature range.[11] At this phase transition only ferroelastic non-180° domain walls are created. On further cooling, SBTO15 transforms at 530 °C from the orthorhombic(I) paraelectric–ferroelastic phase into as orthorombhic(II) ferroelectric–ferroelastic phase. At this phase transition, only ferroelectric 180° domain walls are created within already existing ferroelastic domains structure. A similar intermediate paraelectric phase has recently been described in related $Sr_{0.85}Bi_{2.1}Ta_2O_9$ composition by Hervoches *et al.*[12] Another possible evidence of a high temperature nonferroelectric phase transition in Aurvillius structures has been reported by Jimenez *et al.*[13] where an elastic anomaly was observed above the temperature of the paraelectric–ferroelectric phase transition. Those authors, however, interpreted the elastic anomaly to be of extrinsic and not structural origin.

Because 180° domain walls (associated with the ferroelectric spontaneous polarization) and non-180° domain walls (associated with the ferroelastic spontaneous strain) are created at different temperatures and under different boundary conditions, and because 180° domain

wall structure was in part defined by already existing non-180° domain walls, it was proposed that the final domain wall structure in SBTO15 might be stable under external fields.[11] Therefore, domain-wall displacement under usual, weak-to-moderate fields, is expected to be reduced. It is well known that in ferroelectric ceramics, displacement of non-180° domain walls may lead to both field and frequency dependence of the piezoelectric properties.[14,15] The effective absence of the weak-field domain wall displacement in SBTO15 thus leads to remarkable stability of the piezoelectric response.[14] However, recent results have shown that, under certain processing conditions, a frequency dependent piezoelectric response may be observed in SBTO15-based ceramics[16] while the linearity with respect to the driving field amplitude is preserved. Moreover, the frequency dependence can be either in form of relaxation or retardation, even in samples with the same nomimal composition, but which were prepared under different conditions. This result indicates presence of an extrinsic contribution to the piezoelectric properties of SBTO15 that is possibly fundamentally different from the one observed in widely used $Pb(Zr,Ti)_3$ ceramics. The piezoelectric properties in $Pb(Zr,Ti)O_3$ are controlled by domain wall motion and are dependent both on the driving field frequency and amplitude.[14]

The motivations for this investigation are the following. The absence of domain wall contributions to the piezoelectric response in SBTO15 is intriguing because piezoelectrically active ferroelastic domain walls are present in the material.[11] Since most previous measurements were made at relatively weak fields and at room temperature, a question arises whether under different driving conditions domain walls may move. On the other hand, the observed frequency dependence of the longitudinal piezoelectric coefficient in some SBTO15 samples, in which piezoelectric response is linear with the field, does suggest an additional extrinsic mechanism for piezoelectric dispersion, which is related to processing conditions. Therefore, besides its potential technological interest, SBTO15 appears to be an attractive material for investigation of a number of phenomena that may contribute to the piezoelectricity of ferroelectrics. The present results could thus be of interest not only for understanding piezoelectricity in Aurivillius structures, but in ferroelectric ceramics in general.

II. MATERIAL PREPARATION AND ELECTRICAL MEASUREMENTS

As the properties of SBTO15 are dependent on processing procedure, some details on material preparation are given. $SrCO_3$, Bi_2O_3, and TiO_2 were used as starting raw materials. After milling, the calcination of all oxides and carbonates was performed at temperatures between 850 and 1050 °C for 6 to 14 h. It was found that the calcination occurs in three steps.[9] The first stage below 640 °C is characterized by the reaction of Bi_2O_3 with (i) $SrCO_3$ to form a solid solution, and (ii) part of the TiO_2 to form $Bi_{12}TiO_{20}$. At these temperatures, some TiO_2 remains unreacted. During the second stage, and below 800 °C, the amount of the $SrO–Bi_2O_3$ solid solution and $Bi_{12}TiO_2$ is reduced, and $SrTiO_3$ and $Bi_4Ti_3O_{12}$ are formed. Above 950 °C, $SrTiO_3$ and the remaining $SrO–Bi_2O_3$ solid solution react with BIT to give SBTO15. If calcination is performed at low temperatures, (850 °C), $Bi_4Ti_3O_{12}$ and $SrTiO_3$ can still be found in the calcined powder but disappear during the sintering. Calcination at 1050 °C, with a slow temperature profile,[9] leads to a coarser powder of a single SBTO15 phase. More processing details can be found in Ref. 9.

The samples were sintered in closed crucibles at temperatures between 1220 and 1250 °C for 1 h. These temperatures are lower than those indicated in Sec. III because of the different postion of the thermocouple with respect to the sample during dilatometric measurements described there and during sintering in the furnace. The final relative densities were 92–95%. The full density was taken as 7.44 g/cm^3 from the x-ray diffraction data. Hot forged samples have also been prepared by applying a 20 MPa stress at 1100 °C on prefired pellets (1 h at 1100 °C). The study of SBTO15 sintering was made in a vertical dilatometer in flowing air, on single-phase calcined powder pressed into pellets.

Samples were poled at 200–230 °C under a field of 50 to 90 kV/cm, applied for 10 min. The properties of the ceramics are strongly dependent on the processing conditions. For example, the direct longitudinal d_{33} piezoelectric coefficient of pure SBTO15 could be anywhere in the 10–25 pC/N range, under maximal ppoling conditions for the given sample.

The d_{33} coefficient was measured using a modified Berlincourt-type setup.[14] A sinusoidal [alternating current (ac)] stress with peak-to-peak up to 50 MPa was applied on samples. A mechanical static [direct current (dc)] stress of up to 180 MPa was used to provide the prestress. Both the amplitude and phase angle of the piezoelectrically induced charges were measured as a function of the frequency (0.01–100 Hz) and the applied stress amplitude. The sample temperature was varied between 20 and 200 °C. The amplitude and phase of the dielectric polarization were obtained by applying a sinusoidal electrical field on samples and measuring the resulting charge with a charge amplifier.

III. SINTERING AND MICROSTRUCTURE

The dilatometry experiments show that for all heating rates, the densification of the ceramic is very slow up to a certain temperature and then occurs rapidly. The

dilatometry experiments and scanning electron microscope (SEM) observations of samples at different degrees of densification show three main steps during sintering. They are indicated in Fig. 1. The first stage is characterized by the sintering within agglomerates formed by platelike grains with a similar orientation. At the end of the first stage (approximately 1230 °C), a slowing down of densification occurs because the driving forces to sinter agglomerates together is too small. At the end of this stage, the density is quite low (around 62%). A second stage of densification can be identified when the agglomerates start to reorganize. The relative density obtained at the end of this stage (approximately 1270 °C) is lower than 90% of theoretical. We emphasize again that the temperatures mentioned here are higher than those indicated in Sec. II because of the different position of the thermocouple with respect to the sample during dilatometric measurements described here and during sintering in the furnace. The activation energies for the first (350 kJ/mol) and the second (700 kJ/mol) stage are typical of solid-state mechanisms. No noticeable grain growth occurs during these steps. The grains are typically platelets of thickness 300–500 nm and length 1–4 μm. Colonies of platelets with similar crystallographic orientation result from the sintering of the agglomerates, as shown in Fig. 2.

Above 1270 °C, the sintering accelerates. Because this temperature is independent of the heating rate, the formation of a liquid phase was suspected. Dilatometry experiments showed that samples maintained at this temperature for some time (>5 min) or heated above

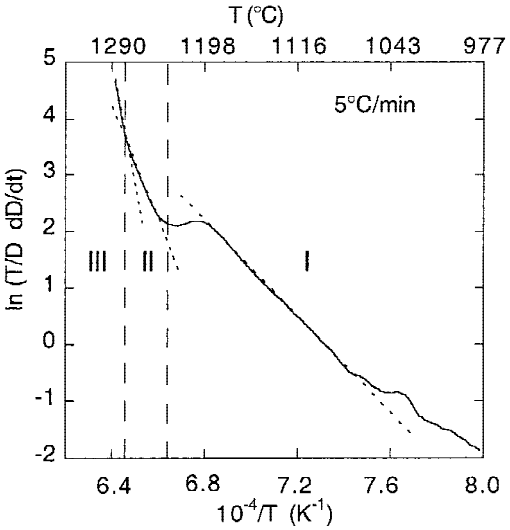

FIG. 1. Densification rate (d*D*/d*t*) versus reciprocal temperature (1/*T*) showing the three main steps of sintering. *D* is the density. Dilatometrical run was carried out at rate 5 °C/min up to 1290 °C. Vertical dashed lines indicate the three densification regions. Inclined dashed lines show slopes at each segment used for calculation of the activation energy.

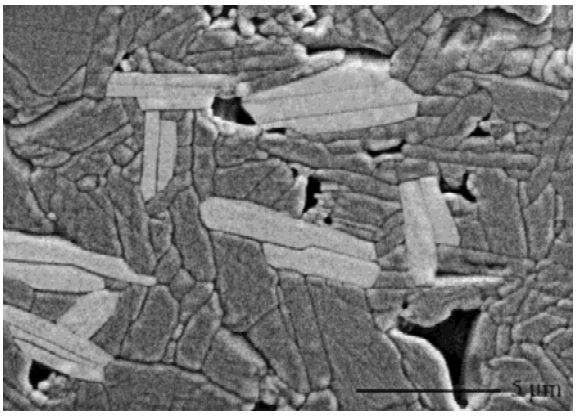

FIG. 2. Typical microstructure of a sample sintered just below the temperature of the liquid phase onset. The highlighted areas show the selected grain colonies creating a local texture.

this temperatures, or for shorter times. This contraction, occurring also when dense samples are reheated above this temperature, is attributed to the freezing of the liquid phase. As x-ray diffraction reveals the presence of $Sr_2Bi_4O_{18}$ (SBTO18) in over-sintered samples, it is likely that part of SBTO15 is decomposed into a Bi-rich liquid phase and SBTO18. It is to be noted that almost no grain growth occurs, unless the sample is maintained for some time at temperatures a few degrees higher than the temperature of apparition of the liquid phase. In that case the thickness of the platelets changes little, but the length increases to more than 10 μm.

Practically, the control of the processing of SBTO15 is difficult, as the material does not densify well below the temperature of the liquid phase formation. The best densities are obtained just below this temperature for rather short times (1–2 hs). We believe that a very small amount of liquid phase helps the sliding and reorganizing of agglomerates, but without allowing changes of microstructure by other mechanism like dissolution–reprecipitation. Longer holds at this temperature lead to apparition of other phases as SBTO18. At lower temperatures the samples are not dense and at higher temperatures a nonnegligible amount of SBTO18 is formed. A difference of 3 to 5 °C in sintering temperature can be significant.

IV. PIEZOELECTRIC PROPERTIES OF SBTO15

A. Field dependence of the piezoelectric properties

The results of structural studies presented in Sec. I suggest that SBTO15 possesses piezoelectrically active non-180° domain walls that, at least under usual experimental conditions, do not contribute significantly to the piezoelectric nonlinearity. The majority of domain walls can therefore be considered trapped in deep

https://doi.org/10.1557/JMR.2002.0205

potential wells, whose exact origin is not known, but could be related to structural reasons as presented in Sec. I and to pinning by the elastic and/or electric defects. If this assumption is correct, one might expect that the domain walls would start moving and contribute to the piezoelectric properties once enough energy is available to overcome the potential barriers. That can be accomplished at high temperatures and under high driving fields where combination of the thermal and field energy may be sufficient to cause small Barkhausen jumps of the walls over the potential barriers. This implies existence of a threshold field above which the piezoelectric response becomes significantly field and frequency dependent due to domain wall displacement.[14]

To investigate this possibility we measured the longitudinal d_{33} piezoelectric coefficient of SBTO15 at room temperature and 150 and 200 °C under very high driving pressure amplitudes. The results are presented in Fig. 3. The nearly linear charge density versus stress response (quasi-constant d_{33}) observed at room temperature is replaced by clear nonlinearity (field-dependent d_{33}) at higher temperatures. Such behavior most likely indicates a thermally activated process assisted by the driving field. To obtain very large dynamic pressures we needed to use samples with a small area on which the alternating force was applied. In our experimental setup, the range of forces that can be generated is limited,[14] so with the smallest dynamic force available, the minimum amplitude of dynamic pressure for these small samples was 10 MPa. As we reported earlier, in the weal field pressure region (from 0.5 to 10 MPa) the d_{33} is, within experimental error, constant with the driving field at all temperatures up to 200 °C.[17] The fact that d_{33} is practically constant at weak dynamic pressures and then starts increasing rather abruptly suggests existence of a threshold field. This abrupt increase in d_{33} as a function of the driving field is dependent on temperature. As indicated by several authors, ferroelectrics usually exhibit some distribution of the coercive fields of individual domains (see for example Refs 18–22). Thus, the threshold fields indicating the onset of dielectric or piezoelectric nonlinearities are rarely sharp and tend to spread over a certain range of applied fields, making their determination somewhat arbitrary. In case of SBTO15, due to relatively small nonlinearity (<6% compared to as much as 50% in $BaTiO_3$ and PZT, or 20% in bismuth titanate[15,23]) and large charge drifts at high temperatures, the data are noisy and threshold fields are even difficult to determine than usual. Assuming certain spread of coercive field for domain walls, we can determine threshold fields at different temperatures in Fig. 3(a) by using the method similar to the one used by Hagemann.[22] In the study of the nonlinear dielectric response of $BaTiO_3$, he defined the threshold field as the field at which nonlinearity reaches a certain level. If we take 2% increase in d_{33} as a reasonable estimate, we find roughly that the apparent threshold field for d_{33} nonlin earity should be around 15–20 MPa at 200 °C, 30–40 MPa at 150 °C, and above 40 MPa at room temperature. The important result is that the onset of the strong nonlinearity (the apparent threshold field) increases with increasing temperature. The same trend would be obtained if we chose another level of nonlinearity as a reference point.

Nonlinearity is accompanied by a piezoelectric hysteresis (Fig. 4) as expected for a response with contribution from domain walls, which move in an energy profile with a distribution of coercive and internal fields.[24] These results are thus consistent with both the presence of non-180° domain walls in SBTO15 and the suggestions that they are trapped but can move irreversibly if enough energy is available. The onset of the strong nonlinearity and d_{33} stress dependence are frequency dependent, as shown in Figs. 3(a) and 3(b). As frequency increases, the onset of the strong nonlinearity is shifted to higher temperatures and higher pressures. Such piezoelectric behavior is in agreement with the one observed in $Pb(Zr,Ti)O_3$

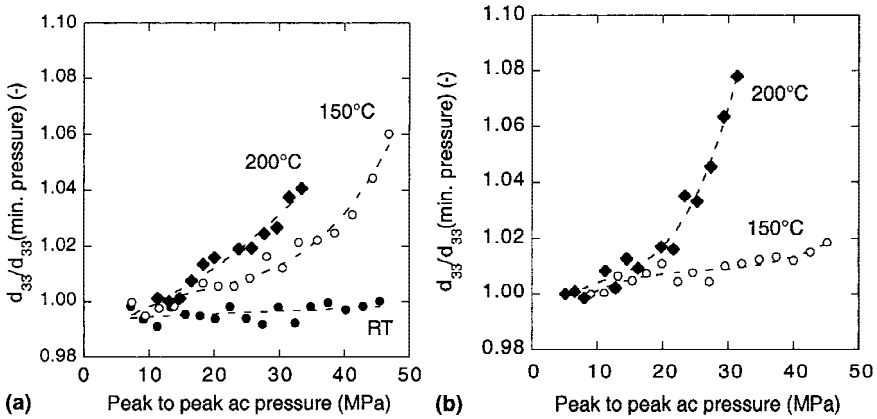

FIG. 3. Relative piezoelectric coefficient versus peak-to-peak as pressure measured at (a) 1 Hz and (b) 10 Hz. The dashed lines are guides for the eye.

https://doi.org/10.1557/JMR.2002.0205

ceramics, where piezoelectric response is dominated by domain wall contributions and where nonlinear piezoelectric parameters were found to be frequency dependent.[14]

B. Frequency dependence of the piezoelectric properties at weak fields

Another interesting feature of the piezoelectric response in SBTO15 is the weak-field frequency dependence of d_{33}, which is not accompanied by the field dependence. In some cases the frequency dependence is observable even at room temperature and always below the threshold field. It was fount that for the same nominal composition, the piezoelectric coefficient could be independent of, increase with, or decrease with the frequency. We refer to both relaxation (increase of d_{33} with frequency) and retardation (decrease of d_{33} with frequency) as relaxation, as is common in the literature on relaxation processes.[25] Such a variety of behaviors should obviously be related to the extremely narrow processing window described in Sec. III. Figures 5 to 7 show different frequency dependence of d_{33} observed for samples prepared at the same time from two batches of powders under the same conditions. Only the sintering parameters were slightly varied, as described below. The piezoelectric measurements were taken at 150 °C. The first sample, sintered in a covered crucible at 1230 °C (relative density 92%) shows almost no change of d_{33} with frequency [Fig. 5(a)] and no hysteresis [Fig. 5(b)]. The second sample, sintered at 1232 °C in a covered crucible (relative density 95%), showed a relaxation (increase of d_{33} with frequency) with a negative phase angle [Fig. 6(a)] and a clockwise sense of the piezoelectric hysteresis rotation [Fig. 6]. A sample sintered at the same temperature without a cover had a lower relative density of 87%, but exactly the same piezoelectric behavior (not shown). A sample sintered without covering at 1235 °C exhibited 90% density and showed retardation [Fig. 7(b)]. The relaxation is temperature dependent; for most samples, the relaxational behavior significant above 150 °C. Similar results have been observed at room temperature for a Mn-doped SBTO15 composition.[16]

A simple model was developed to explain the different relaxation types observed.[26] The platelike microstructure and anisotropy of properties of SBTO15 lead us to consider a model based on piezoelectric composite that consists of two piezoelectric materials placed in series with different dielectric and piezoelectric properties. The longitudinal piezoelectric coefficient d_c of such composite can be written as[26]

$$d_c = \frac{\upsilon_i d_1 \epsilon_2 + \upsilon_2 d_2 \epsilon_1}{\upsilon_2 \epsilon_1 + \upsilon_i \epsilon_2} \quad (1)$$

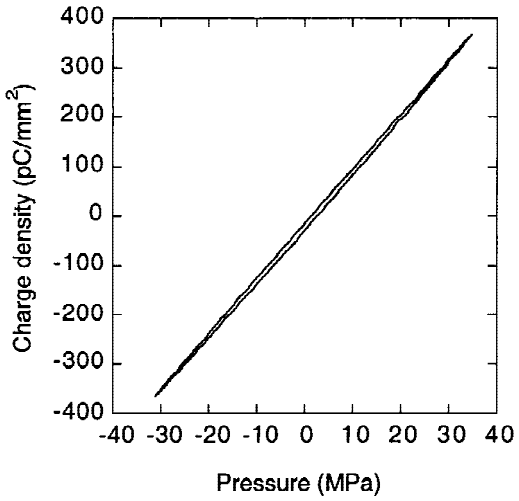

FIG. 4. Charge density versus applied pressure hysteresis at 200 °C, measured at 10 Hz.

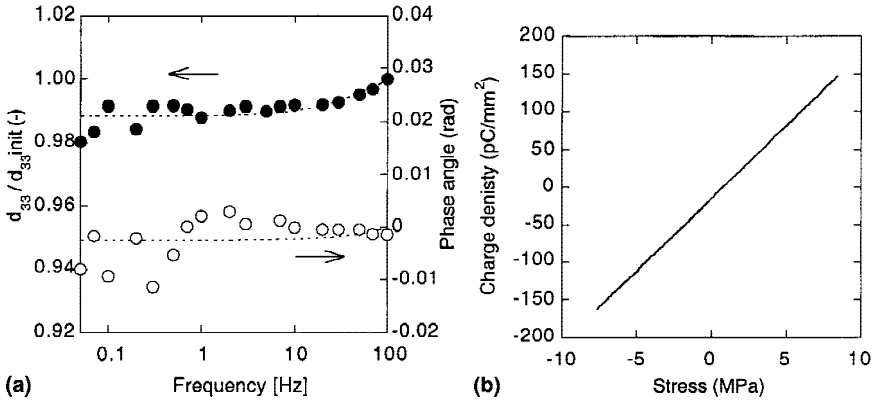

FIG. 5. (a) Relative piezoelectric coefficient (full symbols) and phase angle (open symbols) measured at 150 °C for a sample with relative density 92% sintered in a covered crucible at 1230 °C, illustrating a weak frequency dependence. The dashed lines are guides for eye (b) Nonhysteretic response of the same sample at 0.3 Hz.

https://doi.org/10.1557/JMR.2002.0205

where υ_i is the volume fraction d_i the piezoelectric coefficient, and ϵ_i the permittivity of phase *i*. It is well known that in such a serial system one can easily expect to see Maxwell–Wagner relaxation in the dielectric properties. We have shown that similar effects might contribute to the piezoelectric response of the two phases, in addition to different dielectric, also have different piezoelectric properties.[26] Assuming that the piezoelectric properties of the individual phases are relaxation free, the frequency dependence of d_c can be easily introduced through the frequency-dependent complex permittivity. For example, if the phase i is conducting, then ϵ_i can be replaced by $\epsilon_i' - i\sigma_i/\omega$, where σ_i is the conductivity. More generally, however, one has to take into account additional dielectric relaxation mechanisms and $\epsilon_i = \epsilon_i'(\omega) - i\epsilon_i''(\omega)$. It can be shown that depending on the electrical time constants and piezoelectric coefficients of the two layers, the piezoelectric response may exhibit retardation or relaxation, or be frequency independent.[26] The corresponding imaginary part of the piezoelectric coefficient and the piezoelectric (charge versus pressure) phase angle can then be positive, negative, or zero, and the charge density versus pressure hysteresis can rotate counterclockwise or clockwise, or be absent. The equation the describes the frequency dependence of the serial bilayer composite is given by

$$d_c = d_\infty + \frac{\Delta d}{1+\tau^2\omega^2} - \frac{i\omega\tau\Delta d}{1+\tau^2\omega^2} = d'_{tot}(\omega) - id''_{tot}(\omega) \quad , \tag{2}$$

where $\tau = (\upsilon_1\epsilon_2' + \upsilon_2\epsilon_1')/(\upsilon_i\sigma_2 + \upsilon_2\sigma_1)$ is the relaxation time (the time constant) of the bilayer, $\Delta d = d_0 - d\infty$ is the relaxation strength, $d_0 = (\upsilon_i d_1\sigma_2 + \upsilon_2 d_2\sigma_i)/(\upsilon_i\sigma_2 + \upsilon_2\sigma_i)$ is the static $(\omega \to 0)$ piezoelectric coefficient of the bilayer, and $d\infty = (\upsilon_i d_1\epsilon_2' + \upsilon_2 d_2\epsilon_i')/(\upsilon_i\epsilon_2' + \upsilon_2\epsilon_i')$ is the piezoelectric coefficient at $\omega \to \infty$. Detailed derivation of the equations and their discussion can be found elsewhere.[26] Small changes in the properties of one of the phases can lead to a transition from relaxation to retardation in the same composite. For example, as the ratio of the permittivity and conductivity between the two phases changes with temperature, the relaxation behavior varies.

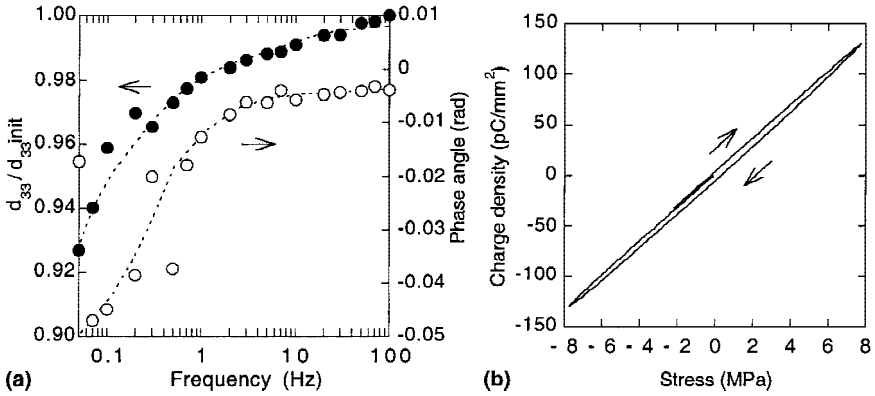

FIG. 6. (a) Relative piezoelectric coefficient (full symbols) and phase angel (open symbols) measured at 150 °C of a sample sintered in a covered crucible at 1232 °C (relative density 95%, showing a relaxation with a negative phase angle. The dashed lines are guides for the eye. (b) Clockwise sense of hysteresis rotation at 0.05 Hz. The arrows indicate hysteresis rotation.

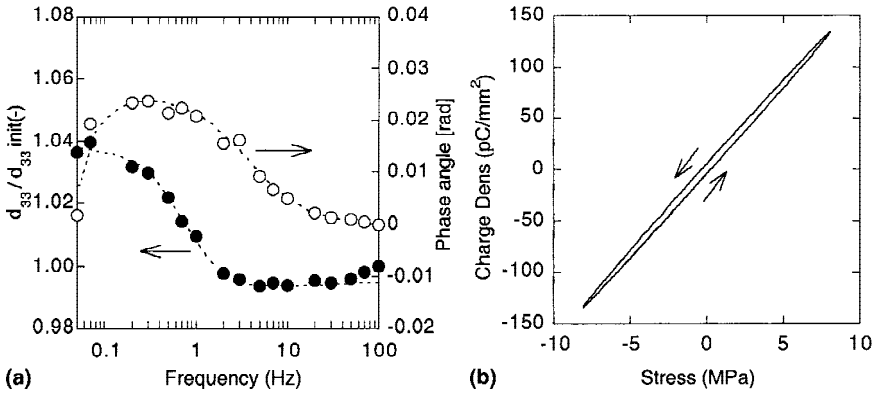

FIG. 7. (a) Relative piezoelectric coefficient (full dots) and phase angle (empty dots) measured at 150 °C of a sample sintered in open air at 1235 °C (relative density 90%), showing retardation and a positive phase angle. The dashed lines are guides for eye. (b) Counterclockwise hysteresis for the same sample at 3 Hz. The arrows indicate hysteresis rotation.

An experimental verification of the model was made on composite made of two different bismuth titanates, $0.88\ Bi_4Ti_3O_{12} + 0.12\ Bi_2Ti_3O_9$ (with $d_{33} = 23$ pC/N, at 1 Hz, and room temperature) and $Bi_2Ti_3O_9 + 0.01\ Bi_2WO_6$ ($d_{33} = 5$ pC/N). These two compositions were chosen since, taken individually, they do not exhibit any frequency dependence of the piezoelectric properties. The two samples had similar thickness and electroded surface areas and thus the volume fraction of each phase was approximately the same. The longitudinal piezoelectric coefficient and dielectric complex permittivity of each sample were measured at selected temperatures and frequencies. The samples were subsequently placed in series and the response of thus-formed composite was measured. Finally, complex d_c of the composite was calculated from the experimental values of individual samples and compared with the direct measurements on the composite. The relations used for calculations are

$$d'_c = \frac{(d_1\epsilon'_2 + d_2\epsilon'_i)(\epsilon'_i + \epsilon'_2) + (d_1\epsilon''_2 + d_2\epsilon''_i)(\epsilon''_i + \epsilon''_2)}{(\epsilon'_i + \epsilon'_2)^2 + (\epsilon''_i + \epsilon''_2)^2}\ , \tag{3}$$

$$d''_c = \frac{(d_1\epsilon''_2 + d_2\epsilon''_i)(\epsilon'_i + \epsilon'_2) - (d_1\epsilon'_2 + d_2\epsilon'_i)(\epsilon''_i + \epsilon''_2)}{(\epsilon'_i + \epsilon'_2)^2 + (\epsilon''_i + \epsilon''_2)^2}\ , \tag{4}$$

$$\mathrm{tg}\delta = d''_c/d'_c\ . \tag{5}$$

Relations (3–5) are obtained from (1), taking $\upsilon_i = \upsilon_2$ and $\epsilon_i = \epsilon'_i(\omega)$ instead of $\epsilon'_i(\omega) - i\sigma_i/\omega$. In most cases, however, we find that the conductivity term dominates and that a satisfactory agreement between calculated and measured results is obtained if we take $\epsilon''_i(\omega) = \sigma_i/\omega$. Figure 8 shows the relaxation behavior of the composite at different temperatures. The calculation using equations (3–4) predicts for d_c retardation at room temperature and relaxation at 150 °C, as is indeed obtained.

To investigate whether anisotropy of the SBTO15 properties can indeed lead to the piezoelectric relaxation, highly textured ceramics were prepared by hot forging, and samples were cut with orientation parallel (*c* oriented) and perpendicular (*ab* oriented) to the forging axis. The piezoelectric coefficient and complex dielectric permittivity of the *ab*-oriented and *c*-oriented SBTO15 samples were measured separately. At 195 °C, the d_{33} for the *ab*-orientation was 27.6 pC/N and 7.8 pC/N for the *c*-oriented sample. For both orientations, there was almost no frequency dependence of d_{33}. A serial composite was then formed of the two samples, and its properties were measured and calculated as described in the example above. Figure 9 shows that under these experimental conditions the composite exhibits relaxation with a negative piezoelectric phase angle and clockwise hysteresis (not shown). The agreement between the measured and calculated values is very good. Therefore, the relaxation observed is not related to domain-wall movement, which under ac pressures used (maximum 15 MPa) are locked, but to piezoelectric Maxwell–Wagner effects.

It is seen from Fig. 2 that agglomerates of platelets with similar orientation sinter together, forming colonies and leading to local texture. Depending on the size, volume fraction and orientation of the colonies and individual grains, their permittivity, conductivity, and piezoelectric response with respect to measurement direction can be very different. The neighboring colonies or grains with different orientation can therefore be considered as basic Maxwell–Wagner units. A ceramic can be considered an assemblage of such units. The total response of the ceramics can be calculated by integrating

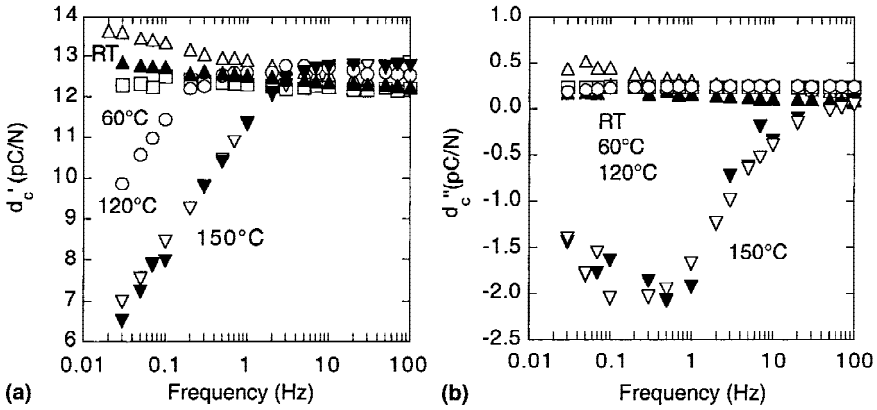

FIG. 8. Relaxation behavior of complex *d* at different temperatures for a composite made of one sample of $0.88Bi_4Ti_3O_{12} + 0.12Bi_2Ti_3O_9$ solid solution (with $d_{33} = 23$ pC/N, at 1 Hz, and room temperature) and one sample of $Bi_2Ti_3O_9 + 0.01Bi_2WO_6$ solid solution ($d_{33} = 5$ pC/N). (a) The real part of *d* and (b) imaginary part of *d* The two samples had approximately the same dimensions and were placed in a series. Open symbols correspond to measurements made at various temperatures, and full symbols are values calculated for the room temperature and 150 °C. Symbol-identification: triangles, room temperature; squares, 60 °C; circles, 120 °C; inverted triangles, 150 °C.

https://doi.org/10.1557/JMR.2002.0205

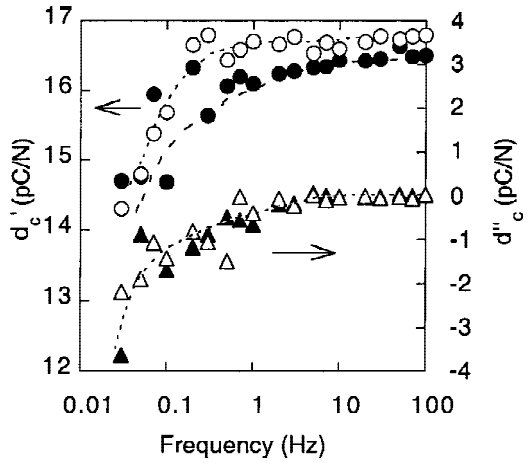

FIG. 9. Real (circles) and imaginary (triangles) part of the piezoelectric coefficient of the SBTO15 hot-forged composite at 190 °C. The open symbols represent measured values on the composite and the full symbols calculated values. The dashed lines are guides for the eye.

contributions from all individual units over all possible orientations and sizes, using the bilayer model as the starting point.

The question arises why the Maxwell–Wagner piezoelectric relaxation is not observed in all ceramics prepared from Aurvillius compounds. If the microstructural anisotropy can induce relaxation, then the characteristic features of the microstructure are an important parameter that controls the relaxation strength. In particular, the aspect ratio and the size of the platelike grains, as well as their agglomeration degree are expected to play a role. To give an example, $Bi_4Ti_3O_{12}$ modified with 20 mol% of Bi_3TiNbO_9 (abbreviated BiTN80/20) is a material that does not show ac stress or frequency dependence of d_{33}.[27] The displacement of piezoelectrically active non-180° domain walls in this material is restricted for structural and microstructural reasons that are discussed elsewhere.[27] A composite made of two pellets cut parallelly and perpendicularly to the *c* axis of hot-forged BiTN80/20 has also been prepared, and a relaxation with negative piezoelectric phase angle was observed in the composite, as in the case of SBTO15. Nevertheless the piezoelectric coefficient of BiTN80/20 ceramics with random grain orientation does not show any relaxation behavior. A closer look at the microstructure reveals that the grains in BiTN80/20 ceramics are smaller (0.5 to 1.5 μm), probably due to presence of niobium. They are also more isotropic-shaped than in SBTO15, and no locally textured zones can be seen.[27] In that case, Maxwell–Wagner effects may be weak, and the piezoelectric response is stable with frequency, at least over the investigated frequency range.

In the case of SBTO15, changes of microstructure due to different processing conditions lead to dramatic changes in the piezoelectric behavior. Samples sintered well below the temperature of appearance of the liquid phase have weakly linked agglomerates. Those samples do not show significant frequency dependence of d_{33} up to 200 °C. Samples sintered for short times at the temperature where densification accelerates show colonies of oriented grains. They behave like a two-phase composite in series and the samples exhibit piezoelectric relaxation. Samples sintered a few degrees above this temperature include additional SBTO18 phase, leading to a complex relaxation behavior that depends on the grain coarsening, appearance of the second phase, and possibly also Bi_2O_3 losses through conductivity modification.

V. CONCLUSIONS

Dynamic piezoelectric measurements showed that non-180° domain walls contribute to the piezoelectric response of strontium bismuth titanate ceramics under high ac pressures, above a certain temperature- and frequency-dependent threshold field. Below this threshold field, $SrBi_4Ti_4O_{15}$ exhibits relaxation and retardation of the piezoelectric properties. The origin of the weak-field frequency dependence of the piezoelectric coefficient is in the high anisotropy of the dielectric and piezoelectric properties in platelike grains that form the ceramic. In ceramics with globally random grain orientation, the number, size, and repartition of the colonies of locally oriented grains are sensitive to processing conditions and this leads to different frequency behavior of the piezoelectric properties in compositions, nominally the same. The frequency dependence of the piezoelectric response of ceramics with random grain orientation can be qualitatively well explained by the piezoelectric Maxwell–Wagner bilayer model.

REFERENCES

1. D. Damjanovic, Current Opinion in Solid State Mater. Sci. **3,** 469 (1998).
2. B.H. Park, B.S. Kang, S.D. Bu, S.D. Noh, J. Lee, and W. Jo, Nature **401,** 682 (1999).
3. B. Aurivilluis, Ark. Kemi. **1,** 499 (1949).
4. R.E. Newnham, R.W. Wolfe, and J.F. Dorrian, Mater. Res. Bull. **6,** 1029 (1971).
5. T. Takenaka and K. Sakata, Jpn. J. Appl. Phys. **19,** 31 (1980).
6. E.C. Subbarao, J. Phys. Chem. Solids. **23,** 665(1962).
7. I.M. Reaney, M. Roulin, H.S. Schulman, and N. Setter, Ferroelectrics **165,** 295 (1995).
8. H.S. Shulman, Ph.D. Thesis, Swiss Federal Institute of Technology—EPFL, Lausanne, Switzerland (1997).
9. C. Voisard, Ph.D. Thesis, Swiss Federal Institute of Technology—EPFL, Lausanne, Switzerland (2000).
10. D. Samjanovic, M Demartin, H.S. Shulman, M. Testorf, and N. Setter, Sens. Actuators A **53,** 353 (1996).
11. I.M. Reaney and D. Jamjanovic, J. Appl. Phys, **80,** 4223 (1996).
12. C. Hervoches, J.T.S. Irvine, and P. Lightfoot, Phys. Rev. B **64,** 100102-1 (2001).

13. B. Jimenez, P. Duran-Martin, R. Jimenez-Rioboo, and R. Jimenez, J. Phys. Conders. Matter **12,** 3883 (2000).
14. D. Damjanovic, J. Appl. Phys. **82,** 1788 (1997).
15. D. Damjanovic and M. Demartin, J. Phys. D: Appl, Phys. **29,** 2057 (1996).
16. M. Demartin Maeder, D. Damjanovic, C. Voisard, P. Duran Mating, and N. Setter, in *Proc, 12th IEEE Int. Symp. on Applications of Ferroelectrics* (IEEE Service Center, Piscataway, NJ) (2000).
17. D. Damjanovic, in *Electroceramics IV*, Vol. 1, edited by R.M. Waser, S. Hoffmann, D. Bonnenberg, and C. Hoffmann (Augustinus Buchhandlung, Aachen, Germany, 1994), pp. 239–246.
18. V. Mueller and Q.M. Zhang, Appl. Phys. Lett. **72,** 2692 (1998).
19. V. Mueller and Q.M. Zhang, J. Appl. Phys. **83,** 3754 (1998).
20. Q.M. Zhang, W.Y. Pan, S.J. Jang, and L.E. Cross, J. Appl. Phys. **64,** 6445 (1988).
21. S. Li, W. Cao, and L.E. Cross, J. Appl. Phys. **69,** 7219 (1991).
22. H.J. Hagerman, J. Phys. C: Solid State Phys. **11,** 3333 (1978).
23. D. Damjanovic and M. Demartin, J. Phys.: Condens. Matter **9,** 4943 (1997).
24. G. Robert, D. Damjanovic, N. Setter, and A.V. Turik, J. Appl. Phys. **89,** 5967 (2001).
25. G.R. Strobl, *The Physics of Polymers* (Springer, Berlin, Germany, 1996).
26. D. Damjanovic, M. Demartin Maeder, C. Voisard, and N. Setter, J. Appl. Phys **90,** 5708 (2001).
27. L. Sagalowicz, F. Chu, P. Duran Martin, and D. Damjanovic, J. Appl. Phys. **88,** 7258 (2001).